J Wood Sci (2003) 49:210–215

ORIGINAL ARTICLE

Hiroshi Yoshihara

Resistance curve for the mode II fracture toughness of wood obtained by the end-notched flexure test under the constant loading point displacement condition

Received: March 15, 2002 / Accepted: July 25, 2002

Abstract The measurement method of mode II fracture toughness-crack propagation length relation (i.e., the resistance curve, or *R*-curve) was examined by end-notched flexure tests on sitka spruce (*Picea sitchensis* Carr.). The tests were conducted by varying the span/depth ratios under the constant loading point displacement condition. The fracture toughness was measured from the load-crack shear displacement (CSD) and load-longitudinal strain relations. The crack length was determined by a combination of load-CSD and load-strain compliances and Williams's end correction theory, as well as the observation of crack propagation. When the specimen had an appropriate span/depth ratio, the fracture toughness and crack propagation length were measured from the load-CSD compliance and combined load-CSD and load-strain compliances, respectively, and the *R*-curve could be determined properly under the constant loading point displacement condition.

Key words Mode II fracture toughness · Crack length · *R*-curve · End-notched flexure test

Introduction

Wooden beams usually contain natural fractures whose planes parallel the longitudinal direction; and bending load is often applied to beams with these fractures. With this loading pattern, fracture often propagates by in-plane shear mode (mode II) or a combination of crack opening (mode I) and in-plane shear modes. Therefore, it is important to measure the mode II fracture toughness properly. When measuring the mode II fracture toughness of advanced composites such as carbon fiber-reinforced plastics (CFRP), the end-notched flexure (ENF) test is commonly performed; its techniques were developed over two decades.[1–5]

In previous studies the ENF test method was examined using western hemlock, and it was found that the testing method could be applied to measuring the fracture toughness of wood under certain testing conditions.[6,7] The ENF tests were conducted under the loading point displacement control condition. Although the crack propagation is not always stable with this loading condition, a servo-controlled testing machine is not required and plural fracture toughnesses can be obtained when the initial crack length is $1/\sqrt[3]{3}\,(\cong 0.693)$ times longer than the half-span. Therefore, the fracture toughness–crack propagation length relation (i.e., the resistance curve, or *R*-curve) can be obtained even in this loading condition. As for the mode II fracture toughness of wood, however, there were few studies of fracture toughness by the *R*-curve because of the difficulty of evaluating the crack length properly. With the ENF test, the crack often propagates obscurely; and the crack length, which has a serious influence on the *R*-curve, is difficult to measure by observation. Kageyama and colleagues proposed the determination method for crack length without observing the crack propagation based on "Williams's end correction theory."[3,4] Nevertheless, Williams's theory requires the elastic constants of the specimen, which should be determined independently of the ENF tests; and there is a concern that the variation in elastic constants inevitably contained in wood cause an incorrect evaluation of crack length. Here a method for determining the mode II *R*-curve of wood is proposed, and the validity of this method was examined.

Theories

Derivation of energy release rate by ENF test

As in Fig. 1, an ENF specimen with a crack length of a is loaded by P at the center of the span of $2L$. The equation for bending is given by the elementary beam theory as follows.

H. Yoshihara (✉)
Faculty of Science and Engineering, Shimane University, 1060 Nishikawazu-cho, Matsue, Shimane 690-8504, Japan
Tel. +81-852-32-6508; Fax +81-852-32-6123
e-mail: yosihara@riko.shimane-u.ac.jp

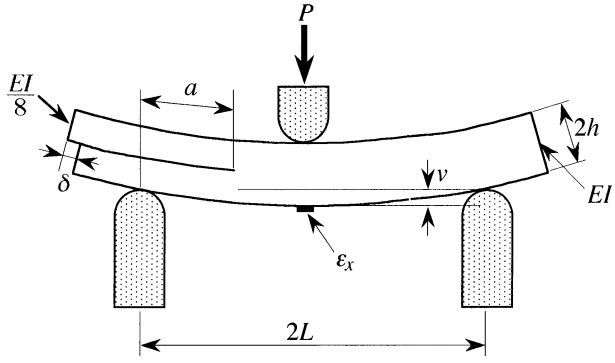

Fig. 1. End-notched flexure (ENF) test

$$\begin{cases} \dfrac{E_x I}{8}\dfrac{d^2y}{dx^2} = -\dfrac{1}{4}Px & \left(0 \le x \le a\right) \\ E_x I\dfrac{d^2y}{dx^2} = -\dfrac{1}{2}Px & \left(a \le x \le L\right) \\ E_x I\dfrac{d^2y}{dx^2} = \dfrac{1}{2}Px - PL & \left(L \le x \le 2L\right) \end{cases} \tag{1}$$

where E_x is Young's modulus in the longitudinal axis, and I is the second moment of cross-sectional area in the crack-free region. Solving this equation, we can obtain the deflection at the loading point v as:

$$v = \frac{P\left(2L^3 + 3a^3\right)}{12E_x I} \tag{2}$$

The loading point compliance C_L is defined as follows.

$$C_L = \frac{v}{P} = \frac{2L^3 + 3a^3}{12E_x I} \tag{3}$$

Hence, the energy release rate in the in-plane shear mode (mode II) , G_{II}, is given as[1,3,4]:

$$G_{II} = \frac{P^2}{2b}\cdot\frac{dC_L}{da} = \frac{9C_L P^2 a^2}{2b\left(2L^3 + 3a^3\right)} \tag{4}$$

where b is the width of the beam. When dG_{II}/da is negative, the crack propagates stably. For stable crack propagation, the crack length a should be larger than $L/\sqrt[3]{3}$ under the constant loading point displacement condition.[1]

Kageyama and colleagues proposed a method for deriving the energy release rate by measuring the crack shear displacement (CSD) instead of measuring the loading point displacement as in Fig. 1.[3] The CSD, denoted as δ, is obtained by integrating the strain along the longitudinal axis from the lower end corner of the upper beam to the crack tip; it is given as follows.

$$\delta = \frac{ha^2}{8E_x I'}P = \frac{ha^2}{E_x I}P \tag{5}$$

where h is the upper beam height of cracked region, and I' is the second moment of cross-sectional area in the cracked region (which equals $I/8$). The CSD compliance C_C is written as follows.

$$C_C = \frac{\delta}{P} = \frac{ha^2}{E_x I} \tag{6}$$

From Eqs. (3)–(6), the energy release rate can be formulated as[3,5]:

$$G_{II} = \frac{P^2}{2b}\cdot\frac{dC_L}{da} = \frac{P^2}{2b}\cdot\frac{3a^2}{4E_x I} = \frac{3P^2 C_C}{8bh} \tag{7}$$

There is a concern that the fracture toughness obtained from Eq. (4) or (7) is influenced by the additional deflection caused by the shearing force that implicitly occurred in the beam.[7] When the longitudinal strain at the most outer plane is measured (Fig. 1), however, the influence of shearing force might be effectively reduced. As in Fig. 1, the longitudinal strain at the midspan ε_x is represented as follows.

$$\varepsilon_x = \frac{Mh}{E_x I} = \frac{PLh}{2E_x I} \tag{8}$$

where M is the bending moment at the midspan. When the load-strain compliance is defined as C_S, it is represented as:

$$C_S = \frac{\varepsilon_x}{P} = \frac{Lh}{2E_x I} \tag{9}$$

From Eqs. (3), (4), and (9), the energy release rate is given as:

$$G_{II} = \frac{P^2}{2b}\cdot\frac{dC_L}{da} = \frac{3P^2 a^2 C_S}{4Lbh} \tag{10}$$

Evaluation of crack length

In the ENF test the crack propagates without a clear opening, and the difficulty evaluating the crack length causes the impropriety of the R-curve even when the fracture toughness is properly measured. To reduce this difficulty, the crack length must be determined without observation. One method for evaluating the crack length is based on Williams's end correction theory. According to that theory, the crack length is regarded as being χh longer than the real length, so the load-CSD compliance C_C is represented as follows.[2]

$$C_C = \frac{h\left(a + \chi h\right)^2}{E_x I} \tag{11}$$

where χ is the function of elastic constants as:

$$\chi = \sqrt{\frac{1}{62.4}\left(\frac{E_x}{G_{xy}}\right)\left\{3 - 2\left(\frac{\sqrt{E_x E_y}}{4.8G_{xy} + \sqrt{E_x E_y}}\right)\right\}^2} \tag{12}$$

where E_y is Young's modulus in the direction of thickness, and G_{xy} is the shear modulus. The crack length evaluated by

the theory is defined as α_w and is determined from Eq. (11) as[3]:

$$\alpha_w = h\left[-\chi + \sqrt{\frac{2bE_xC_C}{3}}\right] \tag{13}$$

With Williams's end correction theory, which was originally applied to measuring the fracture toughness of CFRP by Kageyama and colleagues,[3] measurements of elastic constants are required independently of the ENF tests. Nevertheless, the elastic constants of wood show larger variations than those of CFRP, and there is a concern that these variations cause the impropriety of *R*-curve. Additionally, it is inconvenient to measure the elastic constants independently of the ENF tests. By combining the compliances, however, the crack length during propagation can be calculated without measuring the elastic constants. From Eqs. (3), (6), and (9), the compliance ratios r_{LS}, r_{CS}, and r_{CL} are defined by C_L/C_S, C_C/C_S, and C_C/C_L, respectively, as follows.

$$r_{LS} = \frac{C_L}{C_S} = \frac{L^2\left[2 + 3\left(\frac{a}{L}\right)^3\right]}{6h} \tag{14}$$

$$r_{CS} = \frac{C_C}{C_S} = 2L\left(\frac{a}{L}\right)^2 \tag{15}$$

$$r_{CL} = \frac{C_C}{C_L} = \frac{12h\left(\frac{a}{L}\right)^2}{L\left[2 + 3\left(\frac{a}{L}\right)^3\right]} \tag{16}$$

The ratios at $a = 0.7L$, which is close to the lower boundary for stable crack propagation, are defined as r^0_{LS}, r^0_{CS}, and r^0_{CL}. Figure 2 shows the variances of normalized compliance ratios r_{LS}/r^0_{LS}, r_{CS}/r^0_{CS}, and r_{CL}/r^0_{CL} by crack propagation. As shown in Fig. 2, the variance of r_{CS}/r^0_{CS} is larger than that of the others, which indicates that the value of r_{CS} is more sensitive to the change in crack length than the others. When evaluating the crack propagation length, therefore, it would be effective to use the combination of load-CSD and load-strain compliances and the crack length estimated by the combination of compliances, which is defined as α_c, derived from Eq. (15) as:

$$\alpha_c = \sqrt{\frac{LC_C}{2C_S}} = \sqrt{\frac{Lr_{CS}}{2}} \tag{17}$$

In this experiment, the crack length was evaluated by a, α_w, and α_c. The *R*-curves obtained by the various crack length evaluations were compared with each other.

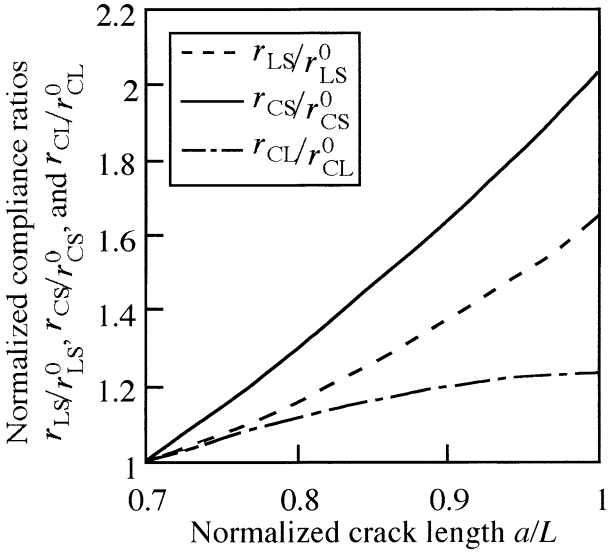

Fig. 2. Variances of normalized compliance ratios by the crack propagation

Experiment

Materials

Sitka spruce (*Picea sitchensis* Carr.), with a density of 0.42 g/cm^3, was used for the specimens. Specimens were conditioned at 20°C and 65% relative humidity (RH) before and during the tests. Five specimens were used for each testing condition.

ENF tests

A beam specimen was cut with the dimensions of 15 × 15 mm in the radial and tangential directions, respectively, and 250–550 mm at intervals of 50 mm in the longitudinal direction. The span length $2L$ varied as 150–450 mm, which was 100 mm shorter than the total length. The crack was initially cut in the longitudinal-tangential plane by a band saw with a thickness of 1 mm; it was then extended by a razor blade. The initial crack length a_0 was 0.7 times the half-span L. A strain-gauge (gauge length 2 mm) (FLA-2-11, Tokyo Sokki, Tokyo, Japan) was bonded to the bottom of the midspan. The crack shear displacement and loading point displacement were measured by the CSD gauge and dial gauge set on the upper cantilever of the specimen and below the loading nose, respectively. Two sheets of Teflon film of 0.5 mm thickness were inserted between the crack surfaces to reduce the friction between the upper and lower cantilever beams. This specimen was supported with the span whose lengths are shown in Table 1, and the load was applied to the midspan of the longitudinal-radial plane not to exceed the strain rate of 0.015/min at the midspan. The loading speed corresponding to the span is shown in Table 1. The load P, crack shear displacement δ, and longitudinal strain at the bottom of the midspan ε_x were measured simultaneously and recorded in a data log at intervals of 2 s.

Table 1. Crosshead speed corresponding to each span and depth

Span $2L$ (mm)	Crosshead speed (mm/min)
150	0.3
200	0.5
250	1.0
300	1.0
350	2.0
400	2.0
450	3.0

The critical load, which is regarded as the load at initiation of crack propagation, was determined to be the load between the straight-line segments through the prelinear and postlinear portions of the load-CSD curves.[6,7] Equation (8) suggests the difficulty of determining the critical load from the load-longitudinal strain relation because this relation has no crack length and is not sensitive to crack propagation. The load-strain relation was used to calculate the energy release rate; hence, the critical load was measured from the load-loading period relation. Prior to the tests, straight lines were drawn in the crack-free region of an LT plane at intervals of approximately $0.03L$ perpendicular to the crack for the specimen. A load was applied until the splitting of a marker line was observed. This process was performed under a magnifying glass. The specimen was then unloaded until a certain load was attained. The specimen was reloaded until the splitting of another marker. This load-unload process was repeated, and the fracture toughness at the beginning of crack propagation G_{IIc} and that during the crack propagation G_{IIR} were calculated from Eqs. (7) and (10). As mentioned above, the crack length was evaluated by a (obtained by observation) and by α_{w} and α_{c} [calculated using Eqs. (13) and (17), respectively]. Plural R-curves corresponding to each span/depth ratio $2L/2h$ were obtained from the various fracture toughness-crack length relations and were compared with each other.

Compression tests

To evaluate the crack length by Williams's end correction theory, α_{w}, Young's moduli E_x and E_y, and the shear modulus G_{xy} were determined by compression tests. Short-column specimens whose dimensions were $60 \times 30 \times 30$ mm were prepared. When measuring E_x and E_y, the long axis of the specimen was male to coincide with the longitudinal and tangential directions of wood, respectively, whereas when measuring G_{xy} the long axis was made to coincide, with its direction inclined at 45° with respect to the grain. Strain-gauges were bonded at the centers of LT planes, and a compression load was applied at a crosshead speed of 0.5 mm/min. Young's moduli were obtained from the stress-strain relation. The shear modulus was determined from the following equation.

$$G_{xy} = \frac{E_{45}}{2(1 + \nu_{45})} \tag{18}$$

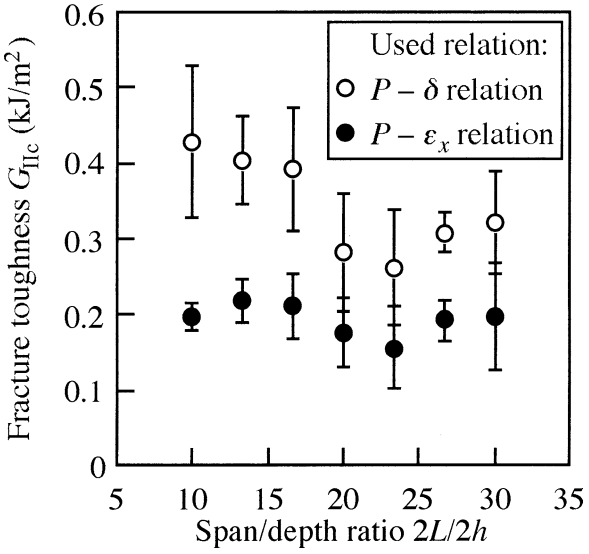

Fig. 3. Fracture toughness at the beginning of crack propagation G_{IIc} corresponding to the initial crack length/half-span $2L/2h$. *Circles* and *horizontal bars* represent the means and standard deviations, respectively

where E_{45} and ν_{45} are Young's modulus and Poisson's ratio in the direction inclined at 45° with respect to the grain, respectively.

Results and discussion

Figure 3 shows the fracture toughness at the beginning of crack propagation G_{IIc} corresponding to the span/depth ratio $2L/2h$. When the span/depth ratio was less than 20, the G_{IIc} value obtained from the load (P)–CSD (δ) relation increased with decreasing span/depth ratio. This tendency was due to the additional crack shear displacement caused by the shearing force.[2] In contrast, G_{IIc} obtained from the load (P)–longitudinal strain (ε_x) relation was rather stable over all span/depth ratios because the longitudinal strain was free from the influence of shearing force. When the fracture toughness was obtained from the P–δ relation, the crack length implicitly contained in Eq. (7) was estimated to be longer than the real one because of the end correction effect shown as Eq. (11), which indicates that the CSD compliance is seriously influenced by this effect. In contrast, the real crack length, in which the end correction effect is ignored, was used when the fracture toughness was calculated from the P–ε_x relation, as in Eq. (10). Because of the corrected crack length, the value of G_{IIc} obtained from the P–δ relation was always larger than that obtained from the P–ε_x relation. This tendency was commonly found in the fracture toughness during crack propagation G_{IIR}. When using the P–ε_x relation for obtaining the fracture toughnesses G_{IIc} and G_{IIR}, there is an advantage in reducing the influence of shearing force. As shown in Eq. (10), however, there is a drawback that the end correction effect cannot be taken into account from the P–ε_x relation. Addi-

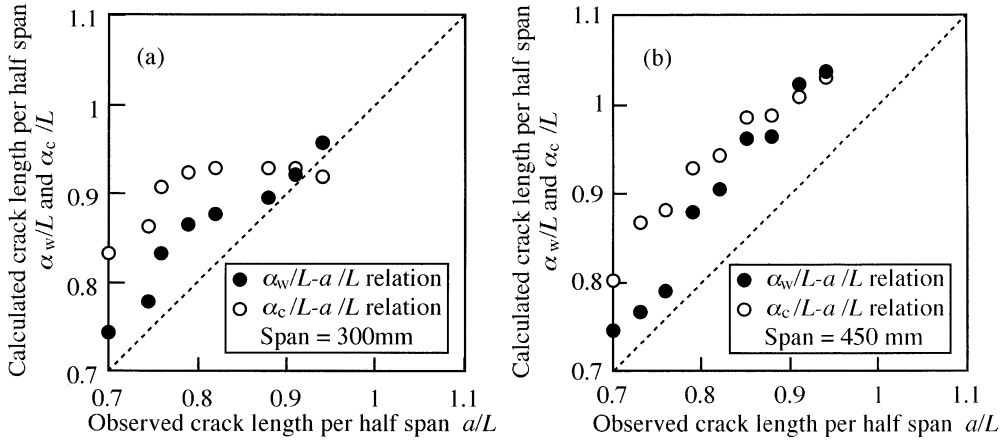

Fig. 4. Crack lengths per half-span calculated from Williams's correction theory and the combination of load-CSD and load-strain compliances corresponding to the observed crack length per half-span. *Open* and *solid circles* were obtained from Williams's correction theory and the combination of compliances, respectively; *dashed line* shows the condition that the calculated crack length is equal to the observed one

tionally, there are two drawbacks when obtaining the value of G_{IIR} from the P–ε_x relation. The first drawback is due to the strain-gauge compliance C_S, which is not essentially changed by the crack propagation, as in Eq. (9). Insensitivity to crack propagation causes incorrect estimation of fracture toughness. The other drawback is due to that the crack length a should be given by the observation when obtaining G_{IIR} from Eq. (10). As mentioned, the crack propagates obscurely in the ENF test, and it is difficult to determine the crack length properly. When determining the fracture toughnesses G_{IIc} and G_{IIR}, use of the P–δ relation by the specimen with an appropriate span/depth ratio is recommended.

Using compression tests, the elastic constants E_x, E_y, and G_{xy} obtained were 12.7, 0.88, and 0.72 GPa, respectively. Substituting these constants into Eqs. (12) and (13), crack length α_w was evaluated by Williams's end correction theory. Figure 4 is an example of the normalized crack lengths α_w/L and α_c/L calculated with Eqs. (13) and (17), respectively, corresponding to the observed crack length normalized by the half span a/L. As shown in Fig. 4b, the tendencies of α_w/L–a/L and α_c/L–a/L relations were similar when the span was larger than 350 mm (span/depth ratio 23.3). This phenomenon indicates that the crack length calculated by the combination of load-CSD and load-strain compliances was as effective as Williams's end correction theory. As shown in Fig. 4a, however, the value of α_c/L did not increase by crack propagation despite the increased α_w/L when the span/depth ratio was small. This tendency was marked when the span was smaller than 300 mm (span/depth ratio 20). The anomalous behavior of α_c/L was caused by the load-strain compliance C_S. Figure 5 shows the normalized strain compliance $C_S I/Lh$ corresponding to the normalized crack length, a/L. Equation (9) suggests that the strain compliance C_S is independent of the crack length, and this independence was verified when the span was larger than 350 mm. When the span was smaller than 300 mm, however, the value of C_S was often increased by crack propagation, as in Fig. 5. When obtaining the R-curve by the combination of load-CSD and load-strain compliances, an appropriate span/depth ratio range exists.

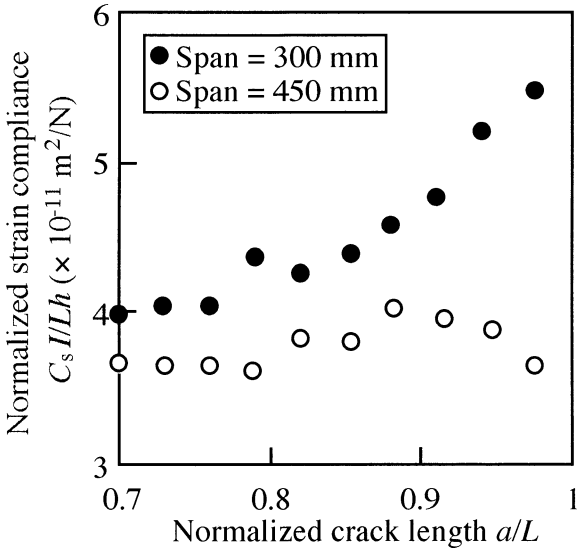

Fig. 5. Variance of normalized strain compliance by crack propagation

Figure 6 shows the R-curves, which are the G_{IIR}-a, α_c, and α_w relations and the G_{IIR}-Δa, $\Delta\alpha_c$, and $\Delta\alpha_w$ relations. The value of G_{IIR} was increased by crack propagation due to "fiber bridgings", which span the upper and lower crack surfaces; and the R-curves showed the convexity whether the crack length was defined by a, α_c, or α_w because the resistance against the crack propagation is increased by the bridgings.[5] As in Fig. 6a, the R-curves obtained using the observed and calculated crack lengths were different from each other. When the fracture toughness and crack propagation length were used as in Fig. 6b, however, the R-curves overlapped.

Considering the difficulty of observing crack propagation and the inconvenience of Williams's end correction theory, the combined compliance method proposed here is appropriate for determining the R-curve. As mentioned above, however, the span/depth ratio should be large enough to reduce the influence of shearing force and to increase strain compliance during crack propagation.

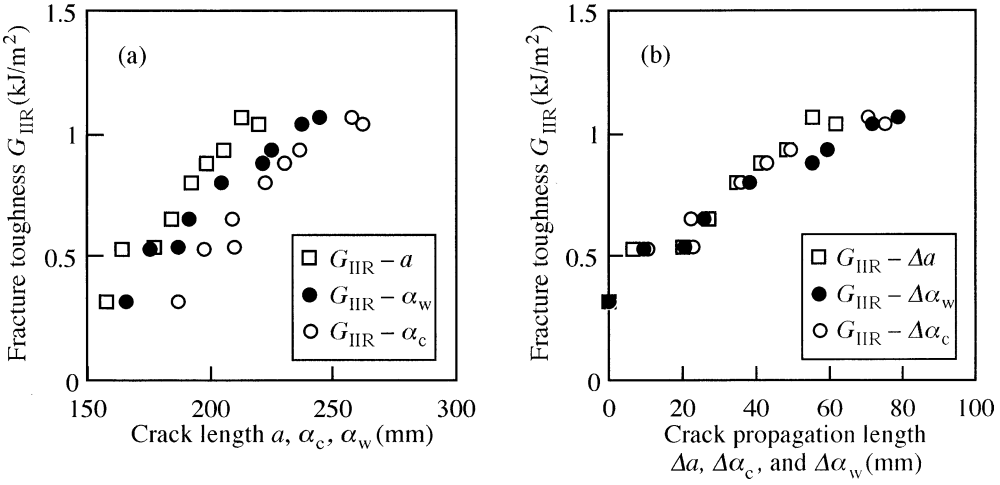

Fig. 6. Comparisons of *R*-curves obtained by various crack length estimations. **a** Fracture toughness-crack length relation. **b** Fracture toughness-crack propagation length relation. Fracture toughness was derived by the load-CSD relation. Span was 450 mm

Conclusions

Using mode II fracture in a spruce specimen, the toughness–crack propagation length relation (*R*-curve) was obtained by the ENF test under the constant loading point displacement condition. The following results were obtained. (1) The fracture toughness obtained by the CSD compliance was influenced by the span/depth ratio because of the shearing force that is inevitable in beam deformation. The fracture toughness obtained by the load-longitudinal strain compliance was free from the influence of shearing force, but it was always smaller than that obtained by the load-CSD compliance because of ignorance of the end correction effect. (2) The crack length, calculated by the combination of load-CSD and load-strain compliances, was close to that derived by Williams's end correction theory when the specimen had an appropriate span/depth ratio. (3) Using the fracture toughness (obtained by the load-CSD compliance) and the crack propagation length (calculated by the combination of load-CSD and load-strain compliances), the *R*-curve can be determined properly under the constant loading point displacement condition.

References

1. Russell AJ, Street KN (1985) Moisture and temperature effects on the mixed-mode delamination fracture of unidirectional graphite/epoxy. ASTM STP 876:349–370
2. Williams JG (1989) The fracture mechanics of delamination tests. J Strain Anal 24:207–214
3. Kageyama K, Kikuchi M, Yanagisawa N (1991) Stabilized end notched flexure test: characterization of mode II interlaminar crack growth. ASTM STP 1110:210–225
4. JIS K7086-1993: testing methods for interlaminar fracture toughness of carbon fibre reinforced plastics
5. Hojo M, Kageyama K (1997) Design and evaluation frontiers of composite materials. V. Fracture mechanics and its properties (in Japanese). J Soc Mater Sci Jpn 46:568–574
6. Yoshihara H, Ohta M (2000) Measurement of mode II fracture toughness of wood by the end-notched flexure test. J Wood Sci 46:273–278
7. Yoshihara H (2001) Influence of span/depth ratio on the measurement of mode II fracture toughness of wood by end-notched flexure test. J Wood Sci 47:8–12